

Material Selection for a Fuel Tank and its FE Simulation in deep drawing

Vijay Gautam¹, Subhajit Konar²

^{1,2}(Department of Mechanical Engineering, Delhi Technological University, Delhi, India)

Vijay.dce@gmail.com, subhokonar94@gmail.com,

Abstract : Deep drawing is a sheet metal forming process in which deformation forces are oriented in plane of the sheet, and the surface pressures in the tool are generally lower than the yield stress of the sheet material. The present work discusses the selection of sheet material suitable for a fuel tank by experimental evaluation of tensile properties of interstitial free steel and deep draw quality steel sheets of the same thickness 0.8mm. The tensile specimens are laser cut from a blank with known rolling direction and are tested for tensile properties and anisotropy. These tensile properties of the sheets are used in material model in FE simulation of the deep draw process using HYPERWORKS. It is observed that an optimum blank holder force is necessary to remove the wrinkling defects. It is concluded that higher ductility and normal anisotropy are the key factors for higher thinning resistance in deep drawing and hence, interstitial free steel sheet qualifies as the better material for the fuel tank.

Keywords: Deep drawing, yield stress, cold rolled draw quality, blank holding force, FE simulation, HYPERWORKS.

I. INTRODUCTION

Deep drawing is very common sheet metal operation used in automobiles, aviation, daily utilities industries etc [1]. Fuel tank is vital part of the automobile which is frequently deep drawn and requires practical testing which incurs cost and time. So it becomes important to develop computational simulation model for finite element analysis of the deep drawing. Jackson et al. [2] recognized the importance of the variation of r-value with orientation in the plane of sheet for low carbon steel. It was reported that the variation in r-values could be exploited for unsymmetrical stampings. The variation of the plastic behavior with direction is assessed by a quantity called Lankford parameter or anisotropy coefficient which is determined by uniaxial tensile tests on sheet specimens in the form of a strip. Zaky et al. [3] presented theoretical results of strain hardening and plastic strain ratio on the limiting draw ratio when drawing with a flat headed punch. It was concluded through experiments that n-value has little effect on limiting draw ratio and while increasing r-value increases the draw ratio. They have shown that at least two instability modes are possible. The first mode in the cup wall occurs under plane strain tension and is most likely to apply to annealed materials. The second mode is in the flange under uniaxial tension and this is most likely to apply to materials that have been previously cold-worked. The limiting drawing ratios for drawing with rough punch are somewhat greater than those for drawing with smooth punch. Darendeliler et al. [4] studied a variable friction model that relates the parameters of sheet metal drawing to the local lubrication conditions taking place during the deformation, integrated to a finite element simulation. Variable friction

coefficients for the contacting surfaces were determined and used in the simulations. Faraji et al. [5] obtained an LDR of 9 for cylindrical components in FE analysis of the multi-stage deep drawing carried out by ABAQUS/explicit FE code. Furthermore, to predict the onset of necking, the forming limit diagram and the forming limit stress diagram were computed and implemented into FE analysis. The best LDRs for each stage were obtained from FE analysis. Gensamer [6] studied the impact of strength and ductility during forming. Improvement in deformation distribution by modification of the plastic properties of substances should be more profitable, when the intrinsic ductility is considerable. However, this should not be true at high strength levels, where intrinsic ductility is low enough to be a more important factor. It is still important for us to try to improve the limiting, local deformation prior to fracture in high strength materials, even though it be of less importance in our more ductile alloys. The process of selection of a material for a fuel tank is quite cumbersome and it requires lot of trial and error methods. Thus it is highly imperative to analyze deep drawing using computational design and modeling techniques.

II. METHODOLOGY

Methodology adopted in the present work is discussed below:

A. Material selection

Two different sheet metals in the annealed state, Interstitial Free steel (IF) and Cold Rolled Deep Draw quality (DDQ) steel of same thickness of 0.8mm were selected in the present work. The chemical composition of the selected materials was determined by spark based spectrometer and the values

are given in Table 1. IF steel sheets are also known as the extra deep draw steel. These are steels from which carbon and nitrogen have been reduced to extremely low levels (less than 0.005%). After vacuum degassing, titanium is added to react with any carbon or nitrogen in solution. Titanium reacts preferentially with sulfur so the stoichiometric amount of titanium that must be added to eliminate carbon and nitrogen is given by: $\%Ti = (48/14)(\%N) + (48/32)(\%S) + (48/12)(\%C)$. These steels have superior formability, ductility and anisotropy which are required for deep drawing operation. Whereas, DDQ steel offers a wide variety of properties including ease of formability, a smooth and clean surface that's why there are mostly used in automobiles, aerospace and other appliances. Annealed coils are lightly rolled by a skinpass mill to prevent a defect called stretcher strain, improve strip shape, and adjust mechanical properties. Skinpass rolling is also used to produce dull finish and bright finish products.

Table 1. Chemical composition of the DDQ & IF steel used (by weight %)

| Steel | C | Si | Mn | Ni | Cr | Cu | V | Al | Ti | S | P |
|-------|----|----|----|----|----|----|----|----|----|----|----|
| D | 0. | 0. | 0. | 0. | 0. | 0. | 0. | 0. | 0. | 0. | 0. |
| D | 05 | 01 | 07 | 03 | 03 | 02 | 01 | 01 | 02 | 02 | 01 |
| Q | 3 | 8 | 6 | 9 | 7 | 2 | 7 | 8 | 5 | 0 | 6 |
| IF | 0. | 0. | 0. | 0. | 0. | 0. | 0. | .0 | 0. | 0. | 0. |
| | 00 | 00 | 11 | 01 | 01 | 00 | 03 | 04 | 04 | 00 | 01 |
| | 4 | 2 | 2 | 2 | 2 | 9 | 6 | 8 | 5 | 9 | 7 |

B. Experimental determination of tensile properties

The specimens as per ASTM standard E8M as shown in Fig. 1 are used for uniaxial tensile testing. The specimens were prepared by CO2 laser in three directions such as parallel (0°), diagonal (45°) and perpendicular (90°) with respect to the rolling direction of the sheet.



Fig. 1. Tensile test specimens in 0°, 45° and 90° w.r.t. the rolling direction

The tensile samples were tested in uniaxial tension in a UTM of 50kN. Load and elongation data were obtained for all the tests and was converted into engineering stress strain data. The standard tensile properties such as yield stress, ultimate tensile stress, uniform elongation and total elongation are determined from the stress- strain plot. The log true stress and log true strain values are calculated in the uniform plastic deformation range (between YS and UTS) and using linear regression (least square method) a best fit was plotted. The slope of this line gives n value and Y- intercept gives log K.

Similarly, plastic strain ratio for both the steels were determined by giving a plastic strain of 20%.

C. Modeling & Simulation

Modeling of the die has been done using the HYPERFORM die module. Initially, the part was modeled in the SOLIDWORKS and split in half along the XY plane. Then the IGES file is created which is further imported to the HYPERFORM die module as shown in Fig. 2.



Fig. 2. Die Face Designed in Die Module

The IGES file of the split part is imported to the HYPERFORM Die Module and geometry clean up is performed to toggle the open edges. After the geometry clean up trim line is created by using create by part option. Then the flat binder is generated and by trimming the binder along the trim line die cavity is created. Similarly, a punch was designed and IGES file data was imported to the die module of HYPERFORM.

A blank of size 410mmX615mm was designed for the deep drawing operation using incremental forming. Two modules of HYPERFORM RADIOSS are used, namely RADIOSS One-Step and Incremental RADIOSS. One-Step is a designer friendly model setup for forming feasibility analysis. The solver is very fast and accurate in predicting the blank shape and forming feasibility early in the product development cycle, minimizing downstream formability challenges and associated costs. Its intuitive nesting interface proposes proper blank-sizing, minimizing material scrap in the early stages of the product development process.

Incremental is the module where actual forming simulation takes place. Here, we setup the deep drawing process, either manually through User Process or automatically through Auto Process. It also has function known as Tool Setup that auto generates punch/die and blank holder meshes from the die/punch mesh using input data such as clearance percentage and blank holding area. The results are viewed and processed in HYPERVIEW.

In this module we can generate binder and punch from the die face designed in the die module section with the suitable percentage clearance between the punch and die. There are two different solvers in this section named as, Incremental RADIOSS and LS-DYNA. Intuitive interface for designers and engineers for quick model setup. Multistage transfer die or progressive die forming modeling using multistage

manager. Supports modeling of single, TWB, Multilayer blanks as shell and solids. Options to create custom process and store it as templates for reuse and share to establish uniform model setup. Fast, Robust, Accurate and Scalable Incremental solver RADIOSS provides quick and best-in-class forming and spring back results. Efficient result interpretation in HYPERVIEW with special tools for forming relevant post processing. The die face as shown in Fig. 3(a) designed using die module is imported in the incremental RADIOSS. Along with this IGES blank file is also imported. Then we go to the mesh>organize>element>components and assign the elements to the die face and blank. Similarly, the punch face is designed as shown in Fig. 3(b).

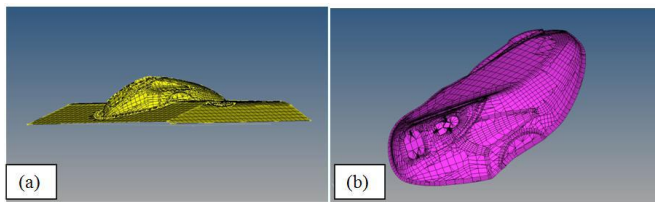


Fig. 3. (a) Die and (b) Punch after meshing

First, the die and blank are meshed and then Tool-Setup function is used to build and setup the punch and binder from die surface. The binder and the blank after meshing is 5

shown in Fig. 4. The Tool Setup function also automatically assigns meshes to punch and binder.

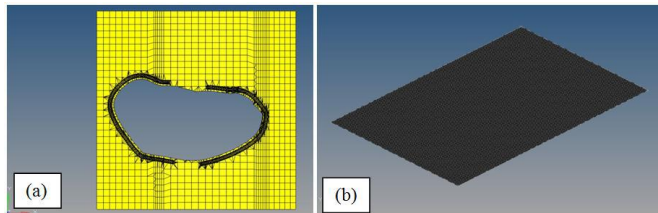


Fig. 4. (a) Binder and (b) Blank after meshing using HYPERMESH

The following figure shows the outcome of the Tool Setup function using die-punch clearance as 10% of sheet thickness. Die, punch and binder are placed such that they just touch the blank surface as shown in Fig. 5.

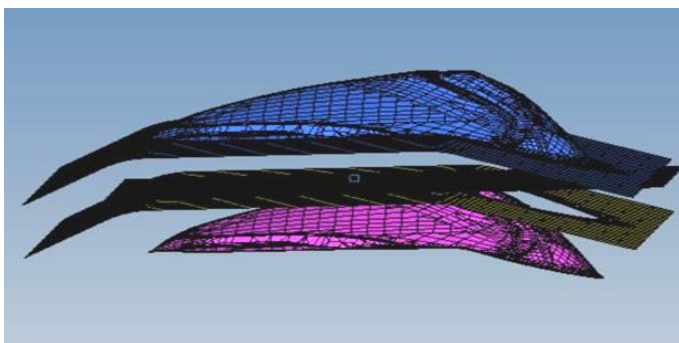


Fig. 5. Assembly of the (1) Die at the top, (2) Blank, (3) Binder and the (4) Punch at the bottom

Die, punch and binder have been assigned rigid meshes known as R-Mesh consisting of four-node shell elements as

they are tools and do not need to be analyzed. Binder has been assigned fine B-Mesh or Belytschko-Tsay shells in order to capture the results with accuracy. After the Tool Setup, User Process is selected in order to finally setup the analysis. We set the material model to be used for sheet.

As this is a double action press, draw, travel and velocity details for punch or die are given in the module. When we click on calculate distance, then it will calculate the travel details. These calculated are automatically fed, with respect to the condition that all other tools just touch the blank. We can also change these values according to our requirements. The final part is drawn in by using 200 KN blank holding force and draw depth of 78mm. The frictional coefficients between various surfaces were taken as 0.125.

III. RESULT AND DISCUSSION

A. Tensile Properties of Materials.

The average tensile properties of the steels samples tested in uniaxial tension tests are given in Table 2. It is observed that the DDQ steel is much stronger than the IF steels with higher UTS and YS, whereas IF steel is softer with highest percentage elongation, strain hardening exponent and normal anisotropy. Therefore, IF steel sheets have higher 6 thinning resistance and deeper components can be drawn easily without necking. Engineering stress and engineering strain plots for the selected samples only are shown in Fig. 6.

Table 2. Tensile properties of steels

| Steel | UTS (MPa) | Yield Stress (MPa) | %EL | Hardness (HRB) | Normal Anisotropy | Strain hardening exponent (n) |
|-------|-----------|--------------------|-------|----------------|-------------------|-------------------------------|
| DDQ | 342 | 186.89 | 44.20 | 69-70 | 1.5 | 0.22 |
| IF | 249 | 110.67 | 47.35 | 30-35 | 2.0 | 0.28 |

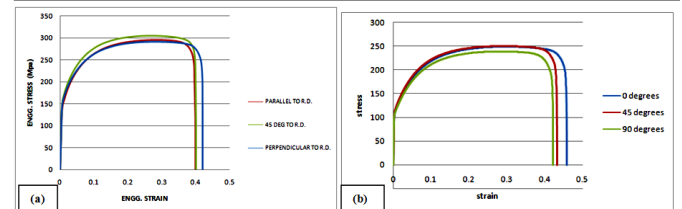


Fig. 6. Engineering Stress and strain plots for (a) DDQ and (b) IF steel sheets

B. Simulation Results.

The simulation results of deep drawing of fuel tank, for the case of IF and DDQ steel with thickness 0.8 mm are shown in Fig. 7(a) and (b) respectively. In the case of IF steel sheets, simulation exhibits the maximum percentage thinning of 26.12% and value of percentage thinning of -18.83%. The equivalent plastic strain remains confined to the upper limit of 0.07633.

From the simulation results of deep drawing of fuel tank for the case of DDQ steel, maximum percentage thinning came out to be 34.89% and minimum value of percentage thinning is -13.10%. The equivalent plastic strain remains confined to the upper limit of the .07588. It is also evident from Forming Limit Diagram (FLD) results as depicted in Fig. 8(a) that in the case of IF steel sheets, there is no failure of material although some wrinkles are developed in the flange region due to circumferential hoop stress which would not be the

part of final component as they would be trimmed in finishing stages.

In the case of DDQ steel, the FLD results as depicted in Fig. 8(b) there is significant necking and failure of material and hence, poor drawability as compared to the IF steel.

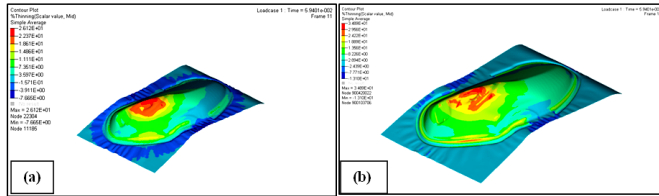


Fig. 7. Thinning contour plots for (a) IF and (b) DDQ steel sheets

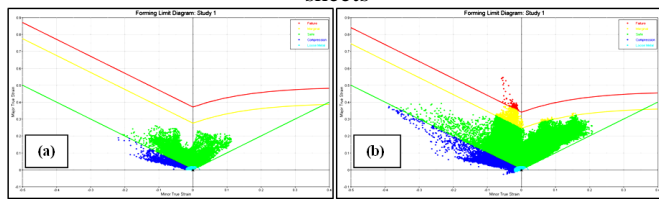


Fig. 8. Forming limit plots for (a) IF and (b) DDQ steel sheets

V. CONCLUSION

The following conclusions are drawn on the basis of the experimental studies and simulations:

- I. DDQ steel is much stronger than the IF steels with higher UTS and YS, whereas IF steel is softer with highest percentage elongation, strain hardening exponent and normal anisotropy. Therefore, IF steel sheets have higher thinning resistance and deeper components can be drawn easily without necking.
- II. In the case of IF steel sheets, simulation exhibits the maximum percentage thinning of 26.12% and value

of percentage thinning of -18.83%. The equivalent plastic strain remains confined to the upper limit of 0.07633.

- III. In the case of DDQ steel, maximum percentage thinning is 34.89% and minimum value of percentage thinning is -13.10%. The equivalent plastic strain remains confined to the upper limit of the 0.07588.

REFERENCES

1. Banabic, D., et al., *Advances in anisotropy and formability*. International Journal of Material Forming, 2010. **3**(3): p. 165-189.
2. Jackson, L., K. Smith, and W. Lankford, *Plastic flow in anisotropic sheet steel*. Am. Inst. Mining. Metall. Eng, 1948. **2440**: p. 1-15. 8
3. Zaky, A., A. Nassr, and M. El-Sebaie, *Optimum blank shape of cylindrical cups in deep drawing of anisotropic sheet metals*. Journal of Materials Processing Technology, 1998. **76**(1): p. 203-211.
4. Darendeliler, H., M. Akkök, and C.A. Yücesoy, *Effect of variable friction coefficient on sheet metal drawing*. Tribology International, 2002. **35**(2): p. 97-104.
5. Faraji, G., M.M. Mashhadi, and R. Hashemi, *Using the finite element method for achieving an extra high limiting drawing ratio (LDR) of 9 for cylindrical components*. CIRP Journal of Manufacturing Science and Technology, 2010. **3**(4): p. 262-267.
6. Gensamer, M., *Strength and ductility*. Metallography, Microstructure, and Analysis, 2017. **6**(2): p. 171-185.